Red Marrow–Absorbed Dose for Non-Hodgkin Lymphoma Patients Treated with ^{177}Lu-Lilotomab Satetraxetan, a Novel Anti-CD37 Antibody–Radionuclide Conjugate

Johan Blakkisrud[1], Ayca Løndalen[2], Jostein Dahle[3], Simon Turner[3], Harald Holte[4], Arne Kolstad[4], and Caroline Stokke[1,5]

[1]Department of Diagnostic Physics, Oslo University Hospital, Oslo, Norway; [2]Department of Radiology and Nuclear Medicine, Oslo University Hospital, Oslo, Norway; [3]Nordic Nanovector ASA, Oslo, Norway; [4]Department of Oncology, Norwegian Radium Hospital, Oslo University Hospital, Oslo, Norway; and [5]Department of Life Science and Health, Oslo and Akershus University College of Applied Sciences, Oslo, Norway

Red marrow (RM) is often the primary organ at risk in radioimmunotherapy; irradiation of marrow may induce short- and long-term hematologic toxicity. ^{177}Lu-lilotomab satetraxetan is a novel anti-CD37 antibody–radionuclide conjugate currently in phase 1/2a. Two predosing regimens have been investigated, one with 40 mg of unlabeled lilotomab antibody (arm 1) and one without (arm 2). The aim of this work was to compare RM-absorbed doses for the two arms and to correlate absorbed doses with hematologic toxicity. **Methods:** Eight patients with relapsed CD37+ indolent B-cell non-Hodgkin lymphoma were included for RM dosimetry. Hybrid SPECT and CT images were used to estimate the activity concentration in the RM of L2–L4. Pharmacokinetic parameters were calculated after measurement of the ^{177}Lu-lilotomab satetraxetan concentration in blood samples. Adverse events were graded according to the Common Terminology Criteria for Adverse Events, version 4.0. **Results:** The mean absorbed doses to RM were 0.9 mGy/MBq for arm 1 (lilotomab+) and 1.5 mGy/MBq for arm 2 (lilotomab−). There was a statistically significant difference between arms 1 and 2 (Student *t* test, $P = 0.02$). Total RM-absorbed doses ranged from 67 to 127 cGy in arm 1 and from 158 to 207 cGy in arm 2. For blood, the area under the curve was higher with lilotomab predosing than without ($P = 0.001$), whereas the volume of distribution and the clearance of ^{177}Lu-lilotomab satetraxetan was significantly lower ($P = 0.01$ and $P = 0.03$, respectively). Patients with grade 3/4 thrombocytopenia had received significantly higher radiation doses to RM than patients with grade 1/2 thrombocytopenia ($P = 0.02$). A surrogate, non–imaging-based, method underestimated the RM dose and did not show any correlation with toxicity. **Conclusion:** Predosing with lilotomab reduces the RM-absorbed dose for ^{177}Lu-lilotomab satetraxetan patients. The decrease in RM dose could be explained by the lower volume of distribution. Hematologic toxicity was more severe for patients receiving higher absorbed radiation doses, indicating that adverse events possibly can be predicted by the calculation of absorbed dose to RM from SPECT/CT images.

Key Words: red marrow–absorbed dose; antibody–radionuclide conjugate; non-Hodgkin lymphoma; ^{177}Lu-lilotomab satetraxetan

J Nucl Med 2017; 58:55–61
DOI: 10.2967/jnumed.116.180471

Radioimmunotherapy, or antibody–radionuclide conjugate (ARC) therapy, uses targeting antibodies linked to a radionuclide, and ARC therapy based on CD20-specific antibodies has been routinely used for treatment of non-Hodgkin lymphoma. ^{177}Lu-lilotomab satetraxetan (previously referred to as ^{177}Lu-DOTA-HH1; trade name, Betalutin [Nordic Nanovector]) is a novel ARC that targets the CD37 antigen expressed on malignant B cells (*1*). Myelosuppression is the main adverse effect of the CD20-based ARC therapies ^{131}I-tositumomab (Bexxar; GlaxoSmithKline) and ^{90}Y-ibritumomab-tiuxetan (Zevalin; Spectrum Pharmaceuticals) and is widely regarded to be a consequence of marrow irradiation (*2,3*). ARCs composed of a CD37 antibody labeled with ^{131}I and a CD20 antibody labeled with ^{177}Lu have also demonstrated hematologic toxicity (*4,5*). Estimating the absorbed dose to the RM is therefore an imperative when a new ARC is studied. Preclinical studies and preliminary phase 1/2a clinical results indicate that myelosuppression is dosage-limiting also for ^{177}Lu-lilotomab satetraxetan (*6,7*).

The distributed nature of the marrow, intricate microstructure, and dependence on sex and age result in dosimetric challenges. Extensive work has resulted in calculation of S values for the skeleton, making dosimetry in accordance with the MIRD scheme possible (*8*). A requirement is then to estimate the activity concentration both in the RM itself and in the surrounding tissues contributing to crossfire dose (*9*). An indirect measuring procedure for RM itself has traditionally been the method of choice, with blood doses being used as a surrogate. There is a growing consensus that this surrogate is suboptimal for ARC therapy dose estimation, mainly given the often-observed lack of correlation with toxicity and deviations found when compared with direct imaging methods (*10–12*). Through imaging of uptake in marrow itself, correlations have been found between absorbed dose and toxic effects (*10,11,13*), and this correlation is better with 3-dimensional modalities such as SPECT or PET than with planar imaging (*14*).

Predosing with unlabeled antibody on the same day as dosing with the radioactive antibody has been shown to be effective at

Received Jul. 1, 2016; revision accepted Aug. 10, 2016.
For correspondence or reprints contact: Caroline Stokke, The Intervention Centre, Oslo University Hospital, P.O. Box 4950, Nydalen, 0424 Oslo, Norway.
E-mail: carsto@ous-hf.no
Published online Sep. 1, 2016.

blocking accessible noncancerous B cells from treatment with ^{131}I-tositumomab (*15,16*). In the present phase 1/2a trial, only patients in arm 1 received predosing with lilotomab. In addition, all patients were pretreated with a larger amount of the anti-CD20 antibody rituximab before ^{177}Lu-lilotomab satetraxetan injection.

The aim of this work was to calculate RM doses using SPECT/CT images of patients receiving treatment with ^{177}Lu-lilotomab satetraxetan and investigate whether predosing with unlabeled lilotomab affects the RM dose. We also investigated the correlation between absorbed doses to RM and hematologic toxicity measured by reduction in thrombocytes and neutrophils.

MATERIALS AND METHODS

Patient Population

Eight patients with relapsed indolent non-Hodgkin lymphoma treated in the phase 1 LYMRIT-37-01 trial were included for RM dosimetry. All patents had received prior chemotherapy (Table 1). Patients with prior external-beam radiation therapy to L2–L4 were excluded. The study was approved by the regional ethical committee, and all patients gave written informed consent. The participants received a single injection of ^{177}Lu-lilotomab satetraxetan and were pretreated with the anti-CD20 antibody rituximab (375 mg/m^2) at 4 wk and 3 wk before injection. In arm 1 the patients received predosing with 40 mg of lilotomab before administration of ^{177}Lu-lilotomab satetraxetan, and in arm 2 they did not.

Hematologic Analyses

Blood samples were collected before administration of ^{177}Lu-lilotomab satetraxetan, several times on day 0, once on each of days 1, 2, 3, 4, and 7, every week thereafter until week 4, and then every 6 mo. The blood samples from the first month were decay-corrected to yield time–activity concentration curves. AUC_{blood}, clearance, and volume of distribution were found analytically after monoexponential curve fitting.

The decrease in thrombocytes and neutrophils at nadir relative to baseline was calculated. Hematologic adverse events (thrombocytopenia and neutropenia) were graded by the Common Terminology Criteria for Adverse Events, version 4.0 (*17*).

Image Acquisition and Probe Measurements

The SPECT/CT imaging protocol has been described previously (*1*). In brief, attenuation- and scatter-corrected SPECT/CT images were acquired approximately 96 and 168 h after injection of ^{177}Lu-lilotomab satetraxetan. Patients 13–15 underwent an additional scan 24 h after injection. Whole-body activity half-lives were determined by anterior and posterior probe measurements at a fixed distance from the patients, at the height of the sternum. The first measurement was performed before the patients voided, within 5 min after injection. Additional measurements were performed 10 min after injection and 4, 24, 96, and 196 h after injection.

Quantification and Dosimetry

Absorbed dose to RM was found both by a surrogate method, using blood and whole-body measurements, and by a method based on SPECT/CT images. The surrogate method was primarily performed for comparison purposes. Both methods include a contribution from the RM itself (self-dose) and a contribution from the remainder of the body (cross-dose). The time-integrated activity coefficient for the remainder of the body is

$$\tau_{RB(patient)} = \tau_{WB(patient)} - \tau_{RM(patient)}, \quad \text{Eq. 1}$$

where WB = whole body and RB = remainder of body. To find $\tau_{WB(patient)}$, time–activity curves were calculated using the geometric

TABLE 1
Characteristics of RM Dosimetry Patients

Patient no.	Sex	Age (y)	Dose (MBq/kg)	Injected activity (MBq)	Pretreatment/ predosing*	Baseline thrombocytes (10^9/L)	Baseline neutrophils (10^9/L)	Prior treatment
1	F	58	10	1,102	R	345	4.5	R×4; R-CHOP×2 plus CHOP×4
13	M	72	15	1,416	R	198	2.1	R-CVP×6; R-bendamustin×6
14	F	70	15	1,013	R	243	2.8	EBRT, 30 Gy; R×4; R-bendamustin×6; R-CHOP×6
15	M	68	10	1,130	R	206	3.6	R-CHOP×6
2	M	58	10	1,036	R + lilotomab	233	2.6	R×8; R×4; chlorambucil×6; R-CHOP×6; EBRT, 30 Gy; R-bendamustin×6; R×2
3	M	50	10	746	R + lilotomab	339	7	Chlorambucil×3; EBRT, 30 Gy; R-galiximab×6; R-CHOP×6; R maintenance
9	M	65	15	1,696	R + lilotomab	298	6.8	R×4
12	F	49	15	1,015	R + lilotomab	268	3.1	Intratumoral R with dendritic cells×3 plus EBRT, 8 Gy; intratumoral R with dendritic cells×2 plus EBRT, 8 Gy; R×4; R-bendamustin×1

*R refers to pretreatment with rituximab; lilotomab refers to predosing with unlabeled antibody.

R = rituximab; CHOP = cyclophosphamide, doxorubicin, vincristine, and prednisone; CVP = cyclophosphamide, vincristine and prednisone; EBRT = external-beam radiotherapy.

mean of the probe measurements, were fitted to monoexponential curves, and were integrated analytically. When patient-specific probe measurements was not available, a mean $\tau_{WB(patient)}$ was used.

SPECT/CT Method

Vertebrae L2–L4 were chosen to quantify activity using SPECT/CT images as previously described for tumors (*1*). The mass of the marrow in L2–L4 was estimated for each patient by drawing a volume of interest defining the interior space of the corpus vertebrae. This volume, $V_{L2-L4(patient)}$, mainly consists of RM, yellow marrow, and trabecular bone. Activity in trabecular bone was assumed to be zero, and a multiplicative correction factor, $1 - f_{TB}$, was applied to the interior volume. The factor f_{TB} was assumed to be 0.135 for male patients and 0.148 for female patients (*18*). The rest of $V_{L2-L4(patient)}$ was assumed to be RM. The RM activity concentration in L2–L4 is then

$$\left[A_{L2-L4(patient)}\right] = \frac{A_{L2-L4(patient)}}{V_{L2-L4(patient)}\ (1 - f_{TB})}, \quad \text{Eq. 2}$$

with $A_{L2-L4(patient)}$ being the activity in L2–L4.

Activity concentration points were fitted by monoexponential curves and integrated analytically, resulting in the RM cumulative activity in L2–L4, $\tilde{A}_{L2-L4(patient)}$. The L2–L4 RM time-integrated activity coefficient and the L2–L4 RM mass, $\tau_{L2-L4(patient)}$ and $m_{L2-L4(patient)}$, can then be written as

$$\tau_{L2-L4(patient)} = \frac{\tilde{A}_{L2-L4(patient)}}{A_{0(patient)}} \quad \text{Eq. 3}$$

and

$$m_{L2-L4(patient)} = V_{L2-L4(patient)}\,(1 - f_{TB}), \quad \text{Eq. 4}$$

with $A_{0(patient)}$ being administered activity.

It was assumed that cumulative concentrations were equal throughout the marrow and that L2–L4 accounted for 6.7% of total RM. Therefore, both $m_{L2-L4(patient)}$ and $\tau_{L2-L4(patient)}$ were scaled by 1/0.067 (*19*). These parameters, together with $\tau_{RB(patient)}$, were used as input to OLINDA/EXM, resulting in the image-derived RM dose, or $D_{RM(SPECT)}$ (*20*).

Surrogate Method

The surrogate RM dosimetry is based on the assumption that the cumulative concentration in RM is proportional to that in blood (*21*). The cumulative concentration in blood is derived from AUC_{blood}. Assuming a proportionality constant of unity, and expressing the whole RM mass with reference RM, reference whole-body mass, and patient whole-body mass as

$$m_{RM(patient)} = \frac{m_{RM(ref)}}{m_{WB(ref)}}\ m_{WB(patient)}, \quad \text{Eq. 5}$$

the time-integrated activity coefficient of RM can be expressed as

$$\tau_{RM(patient)} = \frac{\left[\tilde{A}_{blood}\right]}{A_{0(patient)}}\ m_{RM(patient)}. \quad \text{Eq. 6}$$

Reference values for whole body and RM were taken from OLINDA/EXM for male and female phantoms. $\tau_{RM(patient)}$, $\tau_{RB(patient)}$, and $m_{RM(patient)}$ were used as input in OLINDA/EXM, resulting in dose to RM, or $D_{RM(surrogate)}$.

Statistics

The mean RM dose for arms 1 and 2 was compared using a 2-sided Student *t* test. AUC_{blood}, volume of distribution, and clearance from the blood measurements were also compared for arms 1 and 2 using the same test. The difference in RM dose between the grade 1/2 group and the grade 3/4 group was investigated by a 2-sided Student *t* test. The Pearson test was used to check for correlation between individual RM doses and thrombocyte and neutrophil values at nadir. $D_{RM(SPECT)}$ and $D_{RM(surrogate)}$ were compared with a paired Student *t* test. For all statistical tests, a significance level of 0.05 was used.

RESULTS

Dosimetry was primarily performed using SPECT/CT images; Figure 1 shows SPECT/CT images of the L1–L5 vertebrae of two of the patients. The RM-absorbed dose ranged from 67 to 207 cGy, and even though the patients had been treated with different dose levels (10 or 15 MBq/kg), every patient with predosing received a lower absorbed dose than any patient without predosing (Table 2). The contribution from cross-dose to the total RM dose was 17% maximum for the SPECT/CT-based method. Therefore, introducing the scaling factor 0.067 shifted the final RM-absorbed doses by less than 2%. Figure 2 illustrates the RM doses separated with regard to predosing with lilotomab (corresponding to arms 1 and 2). The mean dose for the predosed group, 0.9 mGy/MBq, was significantly lower than the mean dose for the group without predosing, 1.5 mGy/MBq ($P = 0.02$).

Patients with grade 3/4 thrombocytopenia received a significantly higher RM-absorbed dose than patients with grade 1/2 ($P = 0.02$) (Fig. 3A). Two of the patients, both in arm 2, experienced grade 4 thrombocytopenia 3–6 wk after injection. The difference in RM doses between grade 1/2 and grade 3/4 neutropenia

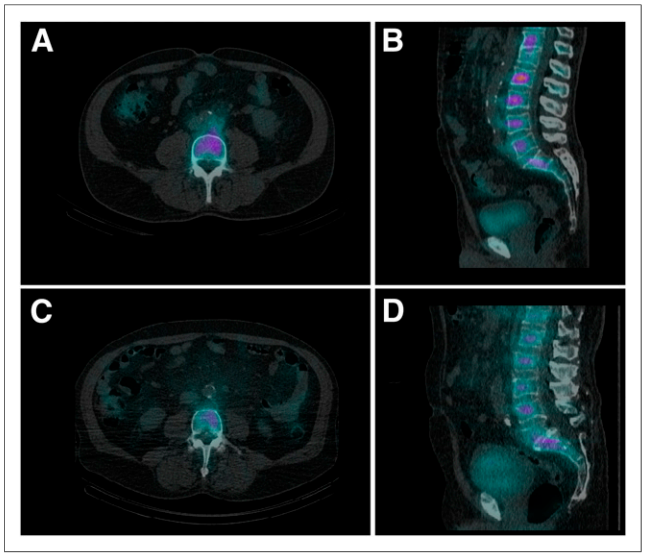

FIGURE 1. (A and B) Axial and sagittal SPECT/CT images of patient 13 at 96 h after ^{177}Lu-lilotomab satetraxetan injection. This patient did not receive predosing with lilotomab. L4 vertebra can be seen in axial slice. Uptake of activity is observed in vertebrae and sacrum; uptake in L2–L4 was quantified and used for RM dosimetry. (C and D) Axial and sagittal SPECT/CT images of patient 9. This patient received predosing with lilotomab.

TABLE 2
RM Doses, Absolute and Normalized

Patient no.	Pretreatment/predosing*	Activity in L2-L4 at 96 h (MBq)	Half-life, 2 time points (d)	Absorbed dose (cGy)	Dose/injected activity (mGy/MBq)
1	R	4.8	3.1	158	1.4
13	R	9.2	1.9 (2.3)	207	1.5
14	R	5.3	3.3 (4.3)	184	1.8
15	R	10.1	3.0	159	1.4
2	R + lilotomab	2.3	6.4	67	0.6
3	R + lilotomab	2.5	4.8	89	1.2
9	R + lilotomab	4.4	4.4	116	0.7
12	R + lilotomab	3.4	2.5	127	1.2

*R refers to pretreatment with rituximab; lilotomab refers to predosing with unlabeled antibody.
Data in parentheses are half-life, 3 time points.

was not statistically significant ($P = 0.39$) (Fig. 3B). There was a moderate, but nonsignificant, linear correlation between the relative reduction in thrombocyte and neutrophil counts at nadir and the RM dose ($P = 0.10$ and $P = 0.11$, respectively) (Figs. 3C and 3D). The CTCAE grade reflects the absolute cell count at nadir. When calculating the correlation between the absolute thrombocyte count and RM dose, a strong and significant linear relationship was found ($r = -0.74$, $P = 0.04$). A moderate to strong but nonsignificant relationship was found for neutrophils ($r = -0.63$, $P = 0.09$).

A higher AUC_{blood} was observed with lilotomab predosing than without ($P = 0.001$) (Table 3). The volume of distribution and the clearance of ^{177}Lu-lilotomab satetraxetan were significantly lower for patients given lilotomab than for those not given lilotomab ($P = 0.01$ and $P = 0.03$, respectively).

The surrogate method resulted in a significant underestimation of RM dose compared with the SPECT/CT-derived dose ($P = 0.002$). The relative difference ranged from 80% to 638%. RM dose calculated by the surrogate method did not show any correlation with hematologic toxicity (Fig. 4).

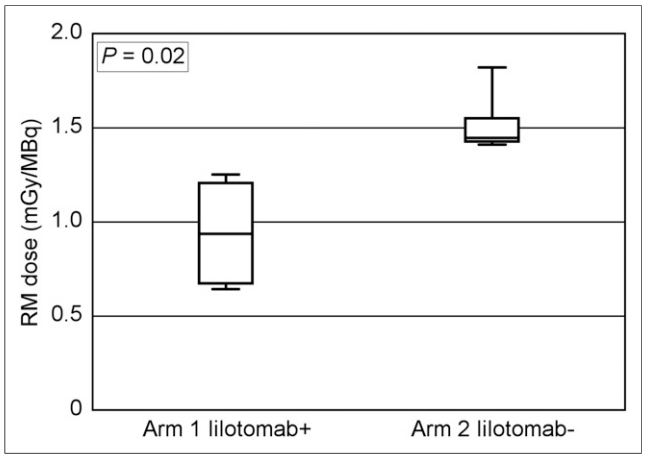

FIGURE 2. RM dose was significantly lower for ^{177}Lu-lilotomab satetraxetan patients in arm 1 than for those in arm 2. Patients in arm 1 received predosing with unlabeled antibody (lilotomab), and patients in arm 2 did not. Absorbed dose is normalized for administered activity.

DISCUSSION

RM is one of the most radiation-sensitive organs in the body. In this work, we have calculated the RM doses and correlated them to hematologic adverse events for 8 patients treated with ^{177}Lu-lilotomab satetraxetan.

The RM doses were significantly higher for arm 2 (lilotomab−) than for arm 1 (lilotomab+). This difference indicates that predosing with lilotomab will have a protective effect on RM, most likely because the unlabeled antibody blocks binding to CD37 in the RM. The activity in blood, AUC_{blood}, was higher and the volume of distribution and clearance were lower for arm 1 than for arm 2, likely because of binding of unlabeled lilotomab to CD37 expressed on cells in the highly perfused compartment, including peripheral blood and RM. This binding by lilotomab to the readily accessible CD37 target antigens then prevents ^{177}Lu-lilotomab satetraxetan from binding to the cells in this compartment, increasing the concentration in the blood, reducing the available volume of distribution, and eventually resulting in reduced amounts of radioactivity in RM. There is a risk that predosing with cold antibody could block the CD37 antigen on tumor tissues as well, but there was no difference in the tumor-absorbed dose between arms 1 and 2 (*1*). This finding might be explained by the reduced distribution volume and clearance in arm 1, because it implies that the concentration of ^{177}Lu-lilotomab satetraxetan was higher for arm 1 patients than for arm 2 patients and the increased concentration will counteract an eventual blocking of CD37 in tumor tissue. The combined findings of these works recommend use of predosing with lilotomab before treatment with ^{177}Lu-lilotomab satetraxetan. The optimal amount of unlabeled antibody has yet to be investigated.

Although the numbers of patients are limited, a clear tendency toward increasing RM dose with patient dose (10 vs. 15 MBq/kg, Table 2) can be seen for each arm. This is in accordance with our finding that absorbed dose in tumors significantly increased with patient dosage level (*1*).

The overall RM dose range was 0.64–1.82 mGy/MBq. This range is of the same order of magnitude as the RM doses listed in the package inserts for ^{90}Y-ibritumomab-tiuxetan and ^{131}I-tositumomab

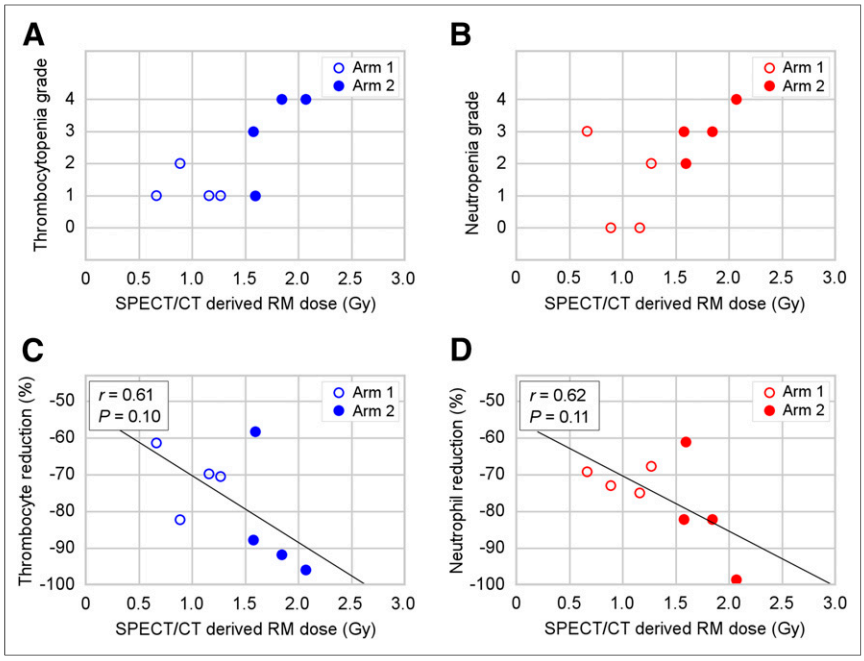

FIGURE 3. Hematologic toxicity vs. RM-absorbed dose for patients receiving ^{177}Lu-lilotomab satetraxetan treatment. (A) Thrombocytopenia grade plotted against dose. Dose was significantly higher for patients with grade 3/4 than grade 1/2 ($P = 0.02$). (B) Neutropenia grade plotted against dose. Higher doses were found for patients with grade 3/4 than grade 1/2, but difference was not statistically significant ($P = 0.39$). (C and D) Relative reduction in thrombocytes (C) and neutrophils (D) at nadir with respect to RM dose.

(*22,23*). Somewhat varying ^{90}Y-ibritumomab-tiuxetan RM doses have been reported, possibly because substitute radioligands have been used for planar imaging and dosimetry (*24,25*). For ^{131}I-tositumomab, the dose is adjusted to produce a 0.75-Gy whole-body dose, shown to correspond to SPECT/CT-derived RM doses of no higher than 1.9 Gy and a median of 1.56 Gy with typical dosage (*26*). Here, RM-absorbed doses for ^{177}Lu-lilotomab satetraxetan are demonstrated to be in accordance with typical dose ranges reported for other ARC treatments.

Clear relationships between RM doses and hematologic toxicity for ARC therapies have traditionally been difficult to establish, and possible explanations include heterogeneous patient groups and dosimetric methodology. In our study, patients developing grade 3/4 thrombocytopenia had received significantly higher RM doses than the grade 1/2 group. For the group-level neutropenia analysis the difference was not significant, and a larger number of patients should be investigated. The need for a larger number is also demonstrated by the absolute neutrophil count and RM dose statistical analyses ($P = 0.09$). Prior chemotherapy, limiting the RM reserve, can also alter the relationship between RM dose and hematologic toxicity (*27*). All patients in our study had undergone prior chemotherapy, with the number of previous treatments ranging considerably (Table 1). Although the limited number of patients prevents quantitative analyses regarding the influence of prior treatments, our findings suggest that the dose–toxicity relationship also depends on the extent of prior chemotherapy. For example, patient 2 had received the most extensive prior treatment, possibly leading to a reduced marrow reserve and explaining the unexpected grade 3 neutropenia after an RM dose of only 67 cGy. In contrast, patient 15, who received an RM dose of 159 cGy, experienced only minor hematologic toxicity. This well-tolerated RM radiation could potentially be explained by the relatively limited prior treatment with only one chemotherapy regime.

Our RM dose calculation relies on the assumption that L2–L4 is representative of the whole marrow. This part of the skeleton has frequently been used, and the resulting doses have shown a correlation with hematologic toxicity (*11,12,19*). Ideally, analyses of all skeletal sites containing RM would strengthen the dosimetry; visual inspection of the SPECT/CT images did, however, suggest similar uptake in other skeletal sites, such as the costae, sacrum, sternum, and ilium. A 2-point dosimetry model was used to avoid introducing systematic errors. An additional time point was available for two patients (patients 13 and 14), and calculations for these 3-point curves demonstrated a low relative difference in RM dose (0% and 8%). For other radionuclide treatments, it has been suggested that calculation of RM doses should be based on the radioactivity concentration in blood, and this method is sometimes also erroneously used to estimate doses for ARCs with specific RM binding. Assuming a conservative estimate of equal activity concentration in blood and RM, we found doses that were between 80% and 638% lower than the SPECT/CT-derived RM doses and no correlation with toxicity (Fig. 4). This finding clearly shows that this surrogate method should not be used to calculate RM doses for patients treated with ^{177}Lu-lilotomab satetraxetan. However, a seemingly inverse proportionality

TABLE 3
Blood Pharmacokinetics

Parameter	Arm 1 ($n = 3$)	Arm 2 ($n = 4$)	P
Dose-adjusted AUC_{blood} (h×[kBq/mL]/[MBq/kg])	661 (31.4)	421 (53.8)	0.001
Volume of distribution (L)	11.7 (1.6)	17.6 (2.8)	0.010
Clearance (mL/h)	148 (28.6)	227 (47.1)	0.029

Data are median followed by SD in parentheses.

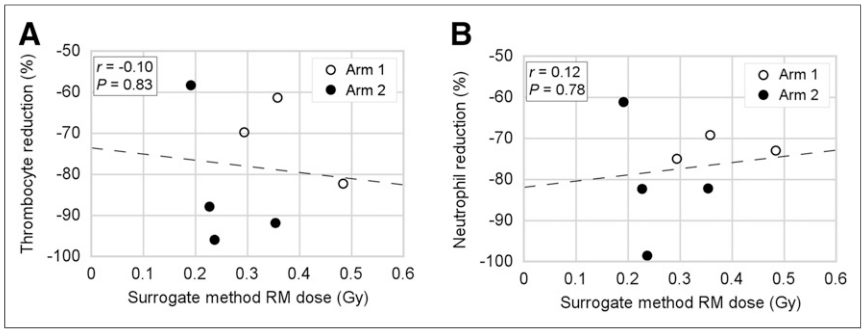

FIGURE 4. Lack of correlation between RM dose derived by surrogate method and reduction in thrombocyte (A) and neutrophil (B) counts demonstrates that this non–imaging-based method is unfit to predict marrow toxicity for ^{177}Lu-lilotomab satetraxetan therapy.

between AUC_{blood} itself and RM dose suggests that alternative models for linking AUC_{blood} and RM dose can possibly be developed.

The reduction in cell count relative to baseline is commonly used to evaluate RM dose against toxicity (*11,13,28,29*). When extrapolating the regression curve in Figures 3C and 3D, we found a 100% reduction of both thrombocytes and neutrophils at 2–3 Gy. Although our data suggest linear regression, sigmoidal fits have been demonstrated in other works, and this 100% reduction dose value should be considered an estimate (*29*). This is further supported by the range in prior chemotherapies for the patient population; this variation can preclude trends for different patient groups. The two patients in our study who experienced grade 4 thrombocytopenia (patients 13 and 14) had received the highest RM doses and were also the only patients receiving an RM dose higher than 1.8 Gy. The widely used 2-Gy dose limit for RM was initially determined for treatment of differentiated thyroid cancer using ^{131}I in the early 1960s (*30*). Later, it was suggested that the potential differences in biologic and physical factors (e.g., dose rate and electron energy) demonstrate a need for empiric determination of dose limits for other novel therapies. Our results support an RM-absorbed dose limit of approximately 2 Gy for patients treated with ^{177}Lu-lilotomab satetraxetan.

CONCLUSION

Although predosing with 40 mg of unlabeled lilotomab significantly reduced the RM-absorbed dose for patients treated with ^{177}Lu-lilotomab satetraxetan, the tumor-absorbed dose was not affected by this amount of unlabeled antibody. These findings support the use of predosing with lilotomab before ^{177}Lu-lilotomab satetraxetan treatment and encourage investigations on the optimal predose, which currently are ongoing. Hematologic toxicity was more severe for patients receiving higher absorbed radiation doses, and our results indicate an RM-absorbed dose limit of about 2 Gy for ^{177}Lu-lilotomab satetraxetan therapy. Given the extent of prior chemotherapy for the population, a somewhat higher dose limit can be expected for patients without such treatment. A surrogate method based on blood sampling instead of imaging demonstrated severe shortcomings for ^{177}Lu-lilotomab satetraxetan treatment. The calculation of RM-absorbed dose, based on SPECT/CT at approximately days 4 and 7, can possibly predict adverse events weeks before they occur. In our experience, such calculations can be performed by trained and prepared personnel within 2 d of the imaging.

DISCLOSURE

This study was sponsored by Nordic Nanovector ASA. Johan Blakkisrud was in part supported by grants from Nordic Nanovector ASA. Arne Kolstad is a member of the Nordic Nanovector Scientific ASA Advisory Board. Both Harald Holte and Arne Kolstad were supported in part by grants from the Norwegian Cancer Society. No other potential conflict of interest relevant to this article was reported.

ACKNOWLEDGMENTS

We thank the personnel at the Nuclear Medicine Section at Oslo University Hospital for technical assistance with the acquisitions. Stine Nygaard, the study nurse at the Department of Oncology, is also greatly acknowledged.

REFERENCES

1. Blakkisrud J, Løndalen A, Martinsen ACT, et al. Tumor absorbed dose for non-Hodgkin's lymphoma patients treated with the novel anti-CD37 antibody radionuclide conjugate ^{177}Lu-lilotomab satetraxetan. *J Nucl Med.* 2017; 58:48–54.
2. Zelenetz AD. A clinical and scientific overview of tositumomab and iodine I 131 tositumomab. *Semin Oncol.* 2003;30:22–30.
3. Jacene HA, Filice R, Kasecamp W, Wahl RL. Comparison of ^{90}Y-ibritumomab tiuxetan and ^{131}I-tositumomab in clinical practice. *J Nucl Med.* 2007;48: 1767–1776.
4. Kaminski MS, Fig LM, Zasadny KR, et al. Imaging, dosimetry, and radioimmunotherapy with iodine 131-labeled anti-CD37 antibody in B-cell lymphoma. *J Clin Oncol.* 1992;10:1696–1711.
5. Forrer F, Oechslin-Oberholzer C, Campana B, et al. Radioimmunotherapy with ^{177}Lu-DOTA-rituximab: final results of a phase I/II study in 31 patients with relapsing follicular, mantle cell, and other indolent B-cell lymphomas. *J Nucl Med.* 2013;54:1045–1052.
6. Repetto-Llamazares AHV, Larsen RH, Mollatt C, Lassmann M, Dahle J. Biodistribution and dosimetry of ^{177}Lu-tetulomab, a new radioimmunoconjugate for treatment of non-Hodgkin lymphoma. *Curr Radiopharm.* 2013; 6:20–27.
7. Kolstad A, Madsbu U, Beasley M, et al. Efficacy and safety results of Betalutin® (177-Lu-DOTA-HH1) in a phase 1/2 study of patients with non-Hodgkin B-cell lymphoma (NHL). Poster presented at: AACR Annual Meeting; New Orleans, Louisiana; 2016.
8. Stabin MG, Eckerman KF, Bolch WE, Bouchet LG, Patton PW. Evolution and status of bone and marrow dose models. *Cancer Biother Radiopharm.* 2002;17:427–433.
9. Hindorf C, Glatting G, Chiesa C, Linden O, Flux G. EANM dosimetry committee guidelines for bone marrow and whole-body dosimetry. *Eur J Nucl Med Mol Imaging.* 2010;37:1238–1250.
10. Boucek JA, Turner JH. Personalized dosimetry of ^{131}I-rituximab radioimmunotherapy of non-Hodgkin lymphoma defined by pharmacokinetics in bone marrow and blood. *Cancer Biother Radiopharm.* 2014;29:18–25.
11. Shen S, Meredith RF, Duan J, et al. Improved prediction of myelotoxicity using a patient-specific imaging dose estimate for non-marrow-targeting ^{90}Y-antibody therapy. *J Nucl Med.* 2002;43:1245–1253.
12. Ferrer L, Kraeber-Bodéré F, Bodet-Milin C, et al. Three methods assessing red marrow dosimetry in lymphoma patients treated with radioimmunotherapy. *Cancer.* 2010;116:1093–1100.
13. Pauwels S, Barone R, Walrand S, et al. Practical dosimetry of peptide receptor radionuclide therapy with ^{90}Y-labeled somatostatin analogs. *J Nucl Med.* 2005;46(suppl 1):92S–98S.

14. Woliner-van der Weg W, Schoffelen R, Hobbs RF, et al. Tumor and red bone marrow dosimetry: comparison of methods for prospective treatment planning in pretargeted radioimmunotherapy. *EJNMMI Phys.* 2015;2:5.
15. Wahl RL. Tositumomab and ^{131}I therapy in non-Hodgkin's lymphoma. *J Nucl Med.* 2005;46(suppl):128S–140S.
16. Kaminski MS, Zasadny KR, Francis IR, et al. Radioimmunotherapy of B-cell lymphoma with [^{131}I]anti-B1 (anti-CD20) antibody. *N Engl J Med.* 1993;329:459–465.
17. *Common Terminology Criteria for Adverse Events.* 4th ed. Bethesda, MD: National Cancer Institute; 2009. NIH publication 09-7473.
18. Schwartz J, Humm JL, Divgi CR, Larson SM, O'Donoghue JA. Bone marrow dosimetry using ^{124}I-PET. *J Nucl Med.* 2012;53:615–621.
19. Herrmann K, Lapa C, Wester H-J, et al. Biodistribution and radiation dosimetry for the chemokine receptor CXCR4-targeting probe ^{68}Ga-pentixafor. *J Nucl Med.* 2015;56:410–416.
20. Stabin MG, Sparks RB, Crowe E. OLINDA/EXM: the second-generation personal computer software for internal dose assessment in nuclear medicine. *J Nucl Med.* 2005;46:1023–1027.
21. Sgouros G. Bone marrow dosimetry for radioimmunotherapy: theoretical considerations. *J Nucl Med.* 1993;34:689–694.
22. Highlights of prescribing information [Zevalin]. Zevalin website. http://www.zevalin.com/downloads/Zevalin_Package_Insert.pdf. Revised August 2013. Accessed September 20, 2016.
23. Highlights of prescribing information [Bexxar]. gsksource website. https://www.gsksource.com/pharma/content/dam/GlaxoSmithKline/US/en/Prescribing_Information/Bexxar/pdf/BEXXAR.PDF. Published 2013. Accessed September 20, 2016.
24. Fisher DR, Shen S, Meredith RF. MIRD dose estimate report no. 20: radiation absorbed-dose estimates for ^{111}In- and ^{90}Y-ibritumomab tiuxetan. *J Nucl Med.* 2009;50:644–652.
25. Wiseman GA, Kornmehl E, Leigh B, et al. Radiation dosimetry results and safety correlations from ^{90}Y-ibritumomab tiuxetan radioimmunotherapy for relapsed or refractory non-Hodgkin's lymphoma: combined data from 4 clinical trials. *J Nucl Med.* 2003;44:465–474.
26. Boucek JA, Turner JH. Validation of prospective whole-body bone marrow dosimetry by SPECT/CT multimodality imaging in ^{131}I-anti-CD20 rituximab radioimmunotherapy of non-Hodgkin's lymphoma. *Eur J Nucl Med Mol Imaging.* 2005;32:458–469.
27. Siegel JA. Update: establishing a clinically meaningful predictive model of hematologic toxicity in nonmyeloablative targeted radiotherapy: practical aspects and limitations of red marrow dosimetry. *Cancer Biother Radiopharm.* 2005;20:126–140.
28. Chiesa C, Botta F, Coliva A, et al. Absorbed dose and biologically effective dose in patients with high-risk non-Hodgkin's lymphoma treated with high-activity myeloablative ^{90}Y-ibritumomab tiuxetan (Zevalin). *Eur J Nucl Med Mol Imaging.* 2009;36:1745–1757.
29. Walrand S, Barone R, Pauwels S, Jamar F. Experimental facts supporting a red marrow uptake due to radiometal transchelation in ^{90}Y-DOTATOC therapy and relationship to the decrease of platelet counts. *Eur J Nucl Med Mol Imaging.* 2011;38:1270–1280.
30. Benua RS, Cicale NR, Sonenberg M, Rawson RW. The relation of radioiodine dosimetry to results and complications in the treatment of metastatic thyroid cancer. *AJR.* 1962;87:171–182.